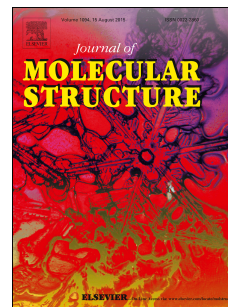


# Journal Pre-proof

Metalation and DFT studies of metal organic frameworks UiO-66(Zr) with vanadium chloride as allyl alcohol epoxidation catalyst

Elham Geravand, Faezeh Farzaneh, Mina Ghiasi



PII: S0022-2860(19)31031-2

DOI: <https://doi.org/10.1016/j.molstruc.2019.126940>

Reference: MOLSTR 126940

To appear in: *Journal of Molecular Structure*

Received Date: 3 June 2019

Revised Date: 22 July 2019

Accepted Date: 17 August 2019

Please cite this article as: E. Geravand, F. Farzaneh, M. Ghiasi, Metalation and DFT studies of metal organic frameworks UiO-66(Zr) with vanadium chloride as allyl alcohol epoxidation catalyst, *Journal of Molecular Structure* (2019), doi: <https://doi.org/10.1016/j.molstruc.2019.126940>.

This is a PDF file of an article that has undergone enhancements after acceptance, such as the addition of a cover page and metadata, and formatting for readability, but it is not yet the definitive version of record. This version will undergo additional copyediting, typesetting and review before it is published in its final form, but we are providing this version to give early visibility of the article. Please note that, during the production process, errors may be discovered which could affect the content, and all legal disclaimers that apply to the journal pertain.

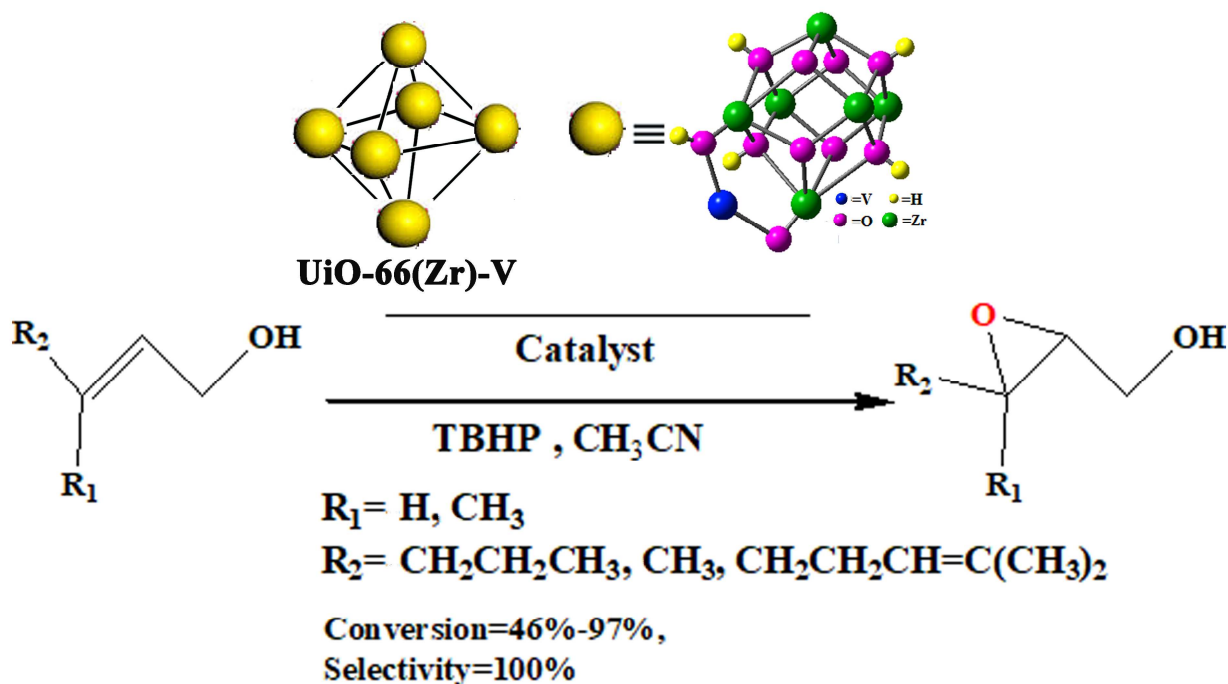
© 2019 Published by Elsevier B.V.

Graphical abstract:

## Metalation and DFT studies of metal organic frameworks UiO-66(Zr) with vanadium chloride as allyl alcohol epoxidation catalyst

Elham Geravand, Faezeh Farzaneh\*, Mina Ghiasi

The metal organic framework UiO-66(Zr)-V was prepared by metalation of the UiO-66(Zr) nodes with  $VCl_3$ . Utilization the density functional theory (DFT) was used in order to find the most stable position of the vanadium of metallated UiO-66(Zr). It was found that UiO-66(Zr)-V has been generated via metalation of V(V) ions with two OH groups of Zr-based nodes. The catalytic activity of UiO-66(Zr)-V on the epoxidation of allyl alcohol is considerable.



**Title page**

**Metalation and DFT studies of metal organic frameworks UiO-66(Zr) with vanadium chloride as allyl alcohol epoxidation catalyst**

**Elham Geravand, Faezeh Farzaneh<sup>\*</sup>, Mina Ghiasi**

*Department of Chemistry, Faculty of Physics & Chemistry, Alzahra University, P.O.Box 1993891176, Vanak, Tehran, Iran*

**\*Corresponding author to: Faezeh Farzaneh,**  
**Tel.:** +98-21-88258977; fax: +98-21-+98-21-88041344;  
E-mail address: [faezeh\\_farzaneh@yahoo.com](mailto:faezeh_farzaneh@yahoo.com), [Farzaneh@alzahra.ac.ir](mailto:Farzaneh@alzahra.ac.ir)

## **Metalation and DFT studies of metal organic frameworks UiO-66(Zr) with vanadium chloride as allyl alcohol epoxidation catalyst**

**Elham Geravand, Faezeh Farzaneh\* , Mina Ghiasi**

*Department of Chemistry, Faculty of Physics & Chemistry, Alzahra University, P.O.Box 1993891176, Vanak, Tehran, Iran*

### **Abstract**

UiO-66(Zr)-V as metal organic framework was prepared by metalation of the UiO-66(Zr) nodes with  $VCl_3$ . The characterization of the prepared catalyst was carried out using XRD, EDX, FT IR, BET, ICP, Raman, DRS, SEM and XPS techniques. The density functional theory (DFT) was used in order to find the most stable position of the vanadium of metallated UiO-66(Zr). It was found that UiO-66(Zr)-V has been generated via metalation of V(V) ions with two OH groups of Zr-based nodes. The XPS results confirmed DFT studies. The catalytic activity of UiO-66(Zr)-V for epoxidation of some allyl alcohols such as trans-2-hexene-1-ol, geraniol, 1-octene-3-ol and 3-methyl-2-buten-1-ol with 46–97% conversions and 100% selectivity is considerable.

**Keywords:** Metal organic frameworks, UiO-66(Zr), Vanadium chloride , allyl alcohols, epoxidation, DFT calculation

---

\*Corresponding author to: **Faezeh Farzaneh,**

**Tel.:** +98-21-88258977; fax: +98-21-+98-21-88041344;

E-mail address: [faezeh\\_farzaneh@yahoo.com](mailto:faezeh_farzaneh@yahoo.com), [Farzaneh@alzahra.ac.ir](mailto:Farzaneh@alzahra.ac.ir)

## 1. Introduction

Inorganic organic hybrid materials include coordination polymers or porous coordination polymers which is designated as metal organic frameworks (MOFs). They are obtained by a combination of metal ions and organic linkers as bridging ligands. Since the synthesis MOF reported by Yaghi and coworkers, more than 70000 MOF have been synthesized [1-4]. Due to their tailorable porosity and higher specific surface. MOFs have been used in various applications such as separation, gas adsorption [5], sensor [6], drug delivery [7], optical luminescence [6] ion exchange [8] and catalysis [6, 9]. They have also been used as acidic and basic catalysts in a variety of organic transformation reactions. Compared to zeolites and other porous materials with a rather high catalytic sites density, MOFs with more available catalytic sites in contact with reacting substances are considerable [10, 11]. Amongst which, zirconium-based MOFs of the UiO-66 family are reported to have exceptional high thermal, chemical and mechanical stability [11, 12]. UiO-66 with  $Zr_6O_4(OH)_4$  octahedral cluster are linked to 12 carboxylates of terephthalate ligands each in three dimensions to form highly porous network [12-14].

Post synthetic modification methods [13] such as modification of surface, linker exchange, metalation and metal exchange have been carried out on many MOFs since their nodes [15] and organic linker sites [16] can be used as support sites.

It is known that missing linkers or ligand defects create accessible Zr-sites in the UiO-66(Zr) framework. In this regard, several experimental techniques have been developed in order to control the amount of open Zr-sites within the UiO-66 material [15]. The stability of the modified UiO-66(Zr) in contact with oxidants such as hydrogen peroxide or TBHP makes it

attractive to be used as oxidation catalyst [15-18]. Recall that epoxidation of allyl alcohols has been the subject of growing interest in the production of chemicals for both industry and academic area because epoxides are widely used as intermediate chemicals in the production of valuable organic and polymer products [19, 20]. Moreover, epoxides have also been applied as precursors for making fine chemicals [21, 22]. Traditionally, transition metal complexes have been used as oxidation catalysts for epoxidation reactions [20]. Example includes vanadium complexes which have been used as catalyst for the epoxidation of alkenes in general and allylic alcohols in particular [19, 23-24]. V-containing MOFs have also been used successfully for some oxidation type reactions [15, 25-26].

In this study, UiO-66(Zr)-V was initially prepared by immobilization of  $VCl_3$  on UiO-66(Zr) and used as heterogeneous catalyst for epoxidation of allyl alcohols. Theoretical study using DFT method was also carried out in order to find the most stable position of V(V) ions within MOF.

## 2. Experimental section

Materials and characterization techniques are reported in supplementary section.

### 2.1. synthesis

#### 2.1.1. Synthesis of UiO-66(Zr)

UiO-66(Zr) was prepared according to the reported procedure [27] with some modification.

See supplementary.

#### 2.1.2. Synthesis of UiO-66(Zr)-V

0.125g (0.8 mmol)  $\text{VCl}_3$  was added to a solution of UiO-66(Zr) (0.086g in 10 mL DMF) and the mixture was then kept at 80 °C for 5 days. The green precipitate was centrifuged, washed with fresh DMF and kept in methanol for 24 h. This procedure was repeated three times. The yellowish green solid was subsequently centrifuged, washed with methanol and dried in a vacuum oven at 100<sup>0</sup> C for 24 h.

## 2.2. Catalytic procedure

In a typical procedure, substrate (10 mmol) and TBHP (12 mmol) were added to the desired amount of catalyst in acetonitrile (5 mL) and the mixture heated at reflux for the appropriate time. Upon completion, the catalyst was collected by filtration on a fine frit, washed with acetonitrile and then dried in an oven. The catalyst was reused at least three times without a significant decrease in catalytic activity or selectivity. The products were identified with GC and GC-Mass techniques.

## 2.3. Computational Scheme

The energy and structural details of all studied compounds including  $[\text{Zr}_6\text{O}_4(\text{OH})_4]$  clusters and the complexes between vanadium and  $[\text{Zr}_6\text{O}_4(\text{OH})_4]$  molecule from different directions have been evaluated using the density functional theory (DFT) [28] without imposing any symmetry constrains. The B3LYP method [29] has been used for the close shell systems. The calculations were performed with standard 6-31+G\* basis set. In the following, some single point calculations using B3LYP/6311+G\*\* to confirm the B3LYP/631+G\* predicted

results have been performed. It is noticeable that DFT methods, are suitable methods for calculations of compounds involving metals. The most impressive advantage of density functional methods is to increase the precision of computational without increasing of computing time.

The frequency calculations have been performed to confirm that an optimized structure refers to local minimum without any imaginary frequencies. Additionally, thermochemistry information including enthalpies and Gibbs energies were evaluated from the frequency calculations at STP conditions. All calculated enthalpies have been corrected with consideration of zero-point energy (ZPE). The solvent effects were investigated using polarized continuum (overlapping spheres) model (PCM) of Tomasi and coworkers [30] at the same level of calculations. All calculations were performed using the Gaussian 2003 [31] software.

### **3. Results and discussion**

Initially, UiO-66(Zr) was prepared as reported before [27]. Subsequently, vanadium chloride immobilized on UiO-66(Zr). The obtained vanadium-MOF with high stability, could be a good candidate as support for many organic transformation reactions.

#### *3.1. Characterization*

##### *3.1.1. XRD Patterns*

The XRD patterns of the prepared UiO-66(Zr) and UiO-66 (Zr)-V are shown in Fig. 1a-b, respectively. Particularly significant is the consistency due to the same crystalline structure since the crystallinity of UiO-66(Zr) did not change after immobilization of vanadium chloride, [12, 15, 32-36]. Observation of a slight reduction in the XRD pattern of peak intensities of the immobilized vanadium on MOF may be due to the slight change in the regular structure of MOF. Therefore, it seems that not only the framework of UiO-66 (Zr) has not been collapsed during the formation of UiO-66 (Zr)-V, but also the crystalline structure of the generated MOF remained intact in the metalation process.

### 3.1.2. SEM and EDX

The morphology of UiO-66(Zr) and UiO-66(Zr)-V determined by SEM revealed the spherical agglomerations [37] of particles in the size of 60-90 nm (Figure S1a,b). On the other hand, comparison of the EDX confirmed the presence of V and Cl atoms on the immobilized UiO-66(Zr) (Fig. 2a, b).

### 3.1.3. FT IR Spectra

The FTIR spectra of UiO-66(Zr) and UiO-66(Zr)-V are shown in Fig. 3a, b, respectively. It was found that all of UiO-66(Zr) framework bands are consistent with those reported in the literature [32, 33] and remained unchanged after deposition of  $VCl_3$  (Fig. 3b).

### 3.1.4. TGA analysis

The UiO-66(Zr) and UiO-66(Zr)-V were examined by thermal gravimetric analysis (TGA) to confirm their thermal and structural identities. The TGA of UiO-66(Zr) exhibited three major weight loss regions (Fig. 4a). The first and the second were attributed to the departure of methanol, and DMF at 28 and 393 °C (18% weight loss), respectively. Whereas removal of methanol was occurred between 25 to 100 °C, the DMF was lost between 100 to 200 °C. The third weight loss region occurred around 400 to 592 °C (38% weight loss) due to the BDC linkers degradation [38].

UiO-66(Zr)-V catalyst showed thermal stabilities slightly less than that of UiO-66 with significant decomposition temperature of approximately 160 to 500 °C framework due to BDC linkers (33% weight loss). Finally, a small weight loss (4% ) at 501 °C was attributed to the oxidation of the vanadium (Fig. 4b) [39].

By comparison of the TGA of UiO-66 and V-UiO66 as well as the reported articles [15], the difference in the thermal stability should be due to the metalation of OH linkers of UiO-66 with vanadium compounds and changing the composition of MOF linkers. Recall that any changes in guest molecule or solvent or coordination of linkers affect the TGA diagrams [15].

### 3.1. 5. Raman spectra

The Raman spectra of UiO-66(Zr) and UiO-66(Zr)-V are shown in Fig. 5 a, b, respectively. It has been shown that the –OH groups on the node of the Zr-based MOFs is metallated with vanadium (V) ions [17].

The Raman spectra of UiO-66(Zr)-V differs with that of UiO-66(Zr) in two bands which appear at 1015 and 1242  $\text{cm}^{-1}$  attributed to V-O-Zr vibrations [15]. The low intensities of these bands are either due to the low percent of vanadium or low density of metalation.

### 3.1.6. $\text{N}_2$ adsorption desorption

$\text{N}_2$  adsorption-desorption isotherms of UiO-66(Zr) and UiO-66(Zr)-V and the obtained related parameters are presented in Fig. 6 and Table 1, respectively. In this study, the adsorption isotherm of UiO-66 is the same as reported previously [40- 43]. As seen in this Table, the surface area was decreased from 1063.19 to the 1019.5 ( $\text{m}^2\text{g}^{-1}$ ). This decrease should be due to the immobilization of vanadium chloride on the surface of UiO-66. The mean pore diameter and total pore volume of UiO-66 (Zr) [33] are observed with rather no change after incorporation of V(V) ions into the SBU clusters. Therefore, the average crystal structure is nearly maintained upon incorporation of V(V) ions (Table 1). Obviously, low decreases in specific surface area of UiO-66(Zr)-V are observed after incorporate of V(V) ions on the UiO-66(Zr) [12] (Table 1). This observation may be due to the fact that the -OH groups on the Zr node of UiO-66(Zr) have also been metallated with V(V) ions. This trend was also observed in the Raman results, accordingly.

### 3.1. 6. XPS

For further analyses of the UiO-66(Zr)-V, chemical status and surface chemical composition. XPS spectra were used as shown in Fig. 7a. The survey scan of UiO-66(Zr)-V indicated the presence of V, Cl, Zr, O and C elements. Fig.7b shows that the binding energies

of Zr  $3d_{5/2}$  and Zr  $3d_{3/2}$  are 182.87 eV and 185.22 eV, respectively. Based on the observed binding energies, the existence of Zr<sup>IV</sup> species in the zirconium-oxo cluster is concluded [37, 44]. On the other hand, the binding energies of V $2p_{3/2}$  and V $2p_{1/2}$  were found to be 517.68 and 525.01 eV [45], respectively (Fig. 7c). A binding energy of 517.68 eV indicates the presence of V(V) species in the UiO-66(Zr)-V [15].

The XPS spectra of O, Zr and V were also measured in order to confirm the existence of a linkage between UiO-66(Zr)-V and VCl<sub>3</sub> molecules. Moreover, deconvolution of binding energy signal of O<sub>1s</sub> into two peaks observed at 531.96 eV and 530.46 eV by Gaussian fitting clearly indicates the presence of O–Zr and O–V bonds in the UiO-66(Zr)-V (Fig. 7d). The presence of chloride was also confirmed by the binding energy peak of Cl<sub>2p</sub> at 199.48 eV (Fig. 7e) [46].

Based on the ICP analysis of UiO-66(Zr), the amount of Zr ions was found to be 28.45%. Moreover, the amount of Zr and V(V) ions in UiO-66(Zr)-V were determined as 27.94% and 5.76%, respectively. It can be concluded that the Zr amount in UiO-66(Zr)-V after metalation has not nearly changed (Table 1).

### 3.1.8. UV spectra

The UV-visible diffuse-reflectance spectrum (DRS) of the UiO-66(Zr), attributed to the adsorption of Zr–O oxoclusters [37] is shown in Figure S2a. The DRS spectrum of UiO-66(Zr)-V also shows two main absorption peaks at 250 to 400 nm and another extra shoulder around 300 to 400 nm due to the V<sup>V</sup> species (Figure S2 b) [15]. As seen in Figure S2 b, the UV-vis absorption edges of the UiO-66(Zr)-V shifted to longer wavelengths in comparison to

that of UiO-66(Zr) upon the incorporation of vanadium chloride into the UiO-66. The absorption peaks observed in the near-visible and the visible regions in the UV-visible spectrum of UiO-66(Zr)-V are mainly attributed to the ligand-to-metal charge transfer [47-48].

The indirect band gap ( $E_g$ ) values of UiO-66(Zr) and UiO-66(Zr)-V were calculated by means of the UV-vis absorption data using the Tauc equation [ $\alpha h\nu = A (h\nu - E_g)^2$ ] [49- 50]. Based on the obtained results, it was found that the grafting of vanadium species decreased the band gap of UiO66 (Zr) from 3.9 to 3.1 eV due to the ligand to metal charge transfer (Figure S3).

### 3.2. Computational studies

#### 3.2.1. Geometry optimization of $[Zr_6O_4(OH)_4]$ cluster

The model system has been used for  $[Zr_6O_4(OH)_4]$  cluster from UiO-66 is constructed using the crystallographic data available in literature [51]. The Comparison between X-ray crystallography data and the optimized geometry of  $[Zr_6O_4(OH)_4]$  cluster are presented in Fig. 8a,b respectively. The optimized structure of cluster of  $[Zr_6O_4(OH)_4]$ , at B3LYP/6-31G\* level without any symmetry constraints is shown in Fig. 8b. The average bond distance between Zr and O atom is 2.28 Å that is in good agreement with X-ray crystallography data, 2.26 Å. A comparison between X-ray [52] data and theoretical results shows that the standard deviation of bond distances, for the B3LYP/6-31G\* is about 0.13 (Table 2).

#### 3.2.2. Interaction between vanadium (V) and $[Zr_6O_4(OH)_4]$ clusters

In order to investigate the position of vanadium on UiO-66 followed to find the most stable position of them, the proposed structures were optimized at B3LYP/6-311++G\*\* level. In the previous reports [15, 17, 51], it was shown that the UiO-66 has missing linkers due to coordination to water and solvent molecules. Huong Giang and co-workers demonstrated that  $V^V$  and  $Ti^{IV}$  can be directly incorporated onto the hexa zirconium oxo hydroxo  $[Zr_6O_4(OH)_4]$  clusters of UiO-66 by reacting with the OH groups especially those that arise from the missing linkers. In the other hand, they indicated five complexes could be formed from connection of  $[Zr_6O_4(OH)_4]$  clusters with vanadium (V) [15, 17]. Besides, they believed that this method of connection between OH groups of UiO-66 and ions could be used for other metal ions. Based on the above mentioned results, in the present research, the five different complexes derived from three clusters linkages of UiO-66 (Fig. 9) designated as Com I, Com II, Com III, Com IV and Com V were studied with (DFT) theory in order to calculate the formation of complexes from different positions and investigate on the stability of five proposed complexes by determination of geometrical details and energetic state of the most thermodynamically stable complex.

As seen in Fig. 9, The  $[Zr_6O_4(OH)_4]$  cluster as A, B, C have bridging OH groups on the node of UiO-66. When the solvent molecules coordinate to sites of the nodes of  $[Zr_6O_4(OH)_4]$  cluster (A), the  $[Zr_6O_4(OH)_4]$  cluster (A) convert to the  $[Zr_6O_4(OH)_4]$  cluster (B and C) with missing linkers. In the  $[Zr_6O_4(OH)_4]$  cluster (B and C), OH groups present at the missing-linker sites of the nodes and could be connected to vanadium ions and formed Com I, Com II, Com III, Com IV and Com V (Figure 9).

The interaction between  $[Zr_6O_4(OH)_4]$  cluster and vanadium in the optimized structures was analyzed. The complexation energy ( $\Delta E_{com}$ ) of five possible complexes were calculated using the equation 1, then the obtained results are given in Table 3.

$$\Delta E_{\text{com}} = E_{\text{opt}} [\text{Zr}_6\text{O}_4(\text{OH})_4]\text{-V} - (E_{\text{opt}} [\text{Zr}_6\text{O}_4(\text{OH})_4] + E_{\text{opt}} \text{V}) \quad (1)$$

The complexation energy was estimated as the difference in energies of isolated  $[\text{Zr}_6\text{O}_4(\text{OH})_4]$  cluster and vanadium (V) ion at their optimized structure, and optimized complex,  $[\text{Zr}_6\text{O}_4(\text{OH})_4]\text{-V}$ .

All calculated thermodynamic functions for the predicted complexes, such as enthalpies ( $\Delta H_{\text{com}}$ ), Gibbs free energies ( $\Delta G_{\text{com}}$ ) and entropies ( $\Delta S_{\text{com}}$ ) are evaluated in the solvents for the most stable complex, Table 3. As the theoretical results indicate the negative  $\Delta E_{\text{com}}$  value for all possible complexes exception of complexes (V) shows the tendency of vanadium ion to interact with the  $[\text{Zr}_6\text{O}_4(\text{OH})_4]$  cluster. As seen in Table 3 and Fig. 10, the stability order of complex of  $[\text{Zr}_6\text{O}_4(\text{OH})_4]\text{-V}$  is Com(I) > Com(II) > Com(III) > Com (IV) > Com(V). To confirm the calculated results and in order to obtain more trusty relative energies the single point calculations at B3LYP/6-311++G\*\* level on different complexes have been done and the same trend have been seen.

Generally, the Gibbs free energy gives the preferential tendency to chemical processes. From the analysis of presented results in Table 3 the following conclusions can be concluded: 1) the complexation of the vanadium from complex (I) in solvent media is more favorable thermodynamically than the other complexes. Details of selected bond distances and bond angles for complex (I) as the most stable complex are given in Table 4, respectively.; 2) The predicted complexation enthalpy values for all possible complexes exception of complexes (V) indicated the exothermic interaction between vanadium and  $[\text{Zr}_6\text{O}_4(\text{OH})_4]$  cluster. The energy level of proposed structures with V are shown in Fig. 10. It should be mentioned the Comp I has been chosen as the most stable one. The good agreement between theoretical and experimental results confirm the predicted results.

### 3. 3. Catalytic study

In order to investigate the catalytic activity of UiO-66(Zr)-V and UiO-66(Zr) for the epoxidation of allyl alcohols with TBHP, trans-2-hexen-1-ol was used as the model substrate. The prepared UiO-66 did not show significant catalytic activity perhaps due to the presence of Zr<sup>IV</sup> in MOF lattice. This result is consistent with those reported before for the low activity of UiO-66 for oxidation type reactions [16]. It was interesting that incorporation of V(V) ions into the UiO-66(Zr) designated as UiO-66(Zr)-V increased the catalytic activity of UiO-66(Zr)-V. Various reaction parameters such as the amount of catalyst, reaction time and solvent were evaluated in order to optimize reaction condition.

Initially, the effect of the catalyst amount on the epoxidation of trans-2-hexene-1-ol was carried out using 10, 30 and 50 mg catalyst within different times in CH<sub>3</sub>CN under reflux condition (Table 5). Therefore, the best catalytic activity was obtained using 30 mg of catalyst within 9 h (Table 5).

To study the effect of solvent on the reaction, epoxidation, of trans-2-hexene-1-ol was carried out within 9 h in either protic or aprotic solvents using 30 mg of catalyst. The obtained results as shown in Fig. 11, indicate that the substrate conversions are higher in aprotic solvents including acetonitrile, dichloromethane, n-hexane and chloroform in comparison to those protic solvents such as methanol and ethanol [52] [Fig. 11]. Therefore, the order of solvent effect of CHCl<sub>3</sub> < n-hexane ~ CH<sub>2</sub>Cl<sub>2</sub> < CH<sub>3</sub>CN is concluded.

In the next step, epoxidation of geraniol, 1-octene-3-ol and 3-methyl-2-buten-1-ol were carried out using CH<sub>3</sub>CN as solvent with 30 mg of catalyst within 1 to 11 h (Table 6, Fig. 12). We have included the epoxidation result of trans-2-hexene-1-ol in Table 6 in order to make

the comparison with other allyl alcohols more convenient. As indicated in Table 6, the four allyl alcohols used in this research afford the corresponding epoxides with 100% selectivities.

Finally, the reusability of UiO-66(Zr)-V as catalyst was investigated in the epoxidation of trans-2-hexen-1-ol. For this, the catalyst of the first run was separated from reaction after completion by centrifuge, washed with acetonitrile and dried before using in the next run. It was found that the catalyst could be reused for three consecutive cycles although a slight decrease in the activity was observed in the third cycle (Fig. 13). Study of the XRD patterns of UiO-66(Zr)-V before and UiO-66(Zr)-V after reaction showed that no change in the structure of UiO-66(Zr)-V catalyst was observed. The XRD patterns of the second and third runs were similar accordingly.

In order to have insight into the reaction mechanism, diphenylamine as a radical scavenger [53] was used in the epoxidation of trans-2-hexen-1-ol. Observation of no inhibition in the epoxidation conversion supports the operation of a concerted oxygen transfer from the oxidant to allyl alcohol substrate. As such, the initial coordination of both allylic alcohol and TBHP to the metal center is followed by oxygen transfer from peroxide to double bond of alcohol via a simultaneous process [19, 24, 25, 54, 55]. Recall that epoxidation reaction is slower in protic solvent since it retards the nucleophilic attack of TBHP to the metal center due to hydrogen bonding. On the other hand, the polarity of aprotic solvent should not be a determining factor in the epoxidation since concerted reaction rates tend not to depend on solvent polarity [56]. As such, a combination of boiling point as well as dielectric constant consistent with the solvent trend exhibited in Figure 11 might be operating.

#### 4. Conclusion

In summary, UiO-66(Zr)-V was prepared by metalation of the UiO-66(Zr) using  $VCl_3$ . The presence of V(V) ions as active site in MOF was proved by means of XPS and ICP. Theoretical calculations were also performed using DFT to study the molecular structure of metalated UiO-66(Zr) with the most stable position of vanadium. In fact, the PXRD patterns of UiO-66(Zr) and UiO-66(Zr)-V have consistency due to the same crystalline structure. Actually, after immobilization of vanadium chloride, the crystallinity did not changed. Compared to the reported articles, the synthesized UiO-66 (Zr) using HCl as modulator contains significant amount of missing-linker defects. In this work, the presence of vanadium metalation via the OH group to UiO-66(Zr) was evidenced. Support for such binding comes from Raman spectrum which shows the presence of V-O-Zr vibration. The ICP as well as XPS results confirm the presence of V(V) in the UiO-66(Zr)-V (V). Therefore, the coordination of V(V) to two oxygens of OH groups was concluded.

Finally, successful epoxidation of four allyl alcohols in moderate to high conversion yields approved the catalytic activity of the prepared MOF. The heterogeneous catalytic activity of the UiO-66(Zr)-V together with stability and reusability for three epoxidation runs with 100% selectivities is promising and its application in the academic area as well as industry is recommended.

## Acknowledgement

The financial support from the Alzahra University is gratefully acknowledged.

## References

- [1] G. Ferey, *Chem. Soc. Rev.* 37 (2008) 191-214.
- [2] P. Deria, J.E. Mondloch, O. Karagiari, W. Bury, J.T. Hupp, O.K. Farha, *Chem. Soc. Rev.* 43 (2014) 5896-5912.
- [3] S. Horike, S. Shimomura, S. Kitagawa, *Nat. Chem.* 1 (2009) 695.
- [4] S. Li, F. Huo, *Nanoscale*, 7 (2015) 7482-7501.
- [5] J.-R. Li, R.J. Kuppler, H.-C. Zhou, *Chem. Soc. Rev.* 38 (2009) 1477-1504.
- [6] R.J. Kuppler, D.J. Timmons, Q.-R. Fang, J.-R. Li, T.A. Makal, M.D. Young, D. Yuan, D. Zhao, W. Zhuang, H.-C. Zhou, *Coord. Chem. Rev.* 253 (2009) 3042-3066.
- [7] A. Ma, Z. Luo, C. Gu, B. Li, J. Liu, *Inorg. Chem. Commun.* 77 (2017) 68-71.
- [8] P. Kumar, A. Pournara, K.-H. Kim, V. Bansal, S. Rapti, M.J. Manos, *Prog. Mater Sci.* 86 (2017) 25-74.
- [9] J. Lee, O.K. Farha, J. Roberts, K.A. Scheidt, S.T. Nguyen, J.T. Hupp, *Chem. Soc. Rev.* 38 (2009) 1450-1459.
- [10] A. Dhakshinamoorthy, A.M. Asiri, H. Garcia, *Chem. Eur. J.* 22 (2016) 8012-8024.
- [11] P. Valvekens, F. Vermoortele, D. De Vos, *Catal. Sci. Technol.* 3 (2013) 1435-1445.
- [12] J.H. Cavka, S. Jakobsen, U. Olsbye, N. Guillou, C. Lamberti, S. Bordiga, K.P. Lillerud, *J. Am. Chem. Soc.* 130 (2008) 13850-13851.
- [13] R.J. Marshall, R.S. Forgan, *Eur. J. Inorg. Chem.* (2016) 4310-4331.
- [14] Y. Bai, Y. Dou, L.-H. Xie, W. Rutledge, J.-R. Li, H.-C. Zhou, *Chem. Soc. Rev.* 45 (2016) 2327-2367.
- [15] H.G.T. Nguyen, N.M. Schweitzer, C.-Y. Chang, T.L. Drake, M.C. So, P.C. Stair, O.K. Farha, J.T. Hupp, S.T. Nguyen, *ACS Catal.* 4 (2014) 2496-2500.
- [16] H. Fei, J. Shin, Y.S. Meng, M. Adelhardt, J. Sutter, K. Meyer, S.M. Cohen, *J. Am. Chem. Soc.* 136 (2014) 4965-4973.
- [17] H.G.T. Nguyen, L. Mao, A.W. Peters, C.O. Audu, Z.J. Brown, O.K. Farha, J.T. Hupp, S.T. Nguyen, *Catal. Sci. Technol.* 5 (2015) 4444-4451.
- [18] K. Leus, P. Concepcion, M. Vandichel, M. Meledina, A. Gorrane, D. Esquivel, S. Turner, D. Poelman, M. Waroquier, V. Van Speybroeck, G. Van Tendeloo, H. Garcia, P. Van Der Voort, *RSC Adv.* 5 (2015) 22334-22342.

- [19] L. Hamidipour, F. Farzaneh, *C. R. Chim.* 17 (2014) 927-933.
- [20] K.A. Joergensen, *Chem. Rev.* 89 (1989) 431-458.
- [21] J.B. Sweeney, *Synthesis of Aziridines*, in: *Aziridines and Epoxides in Organic Synthesis*, Wiley-VCH Weinheim, (2006) 117-144.
- [22] X.H. Lu, Q.H. Xia, H.J. Zhan, H.X. Yuan, C.P. Ye, K.X. Su, G. Xu, *J. Mol. Catal. A: Chem.* 250 (2006) 62-69.
- [23] F. Farzaneh, Y. Sadeghi, M. Maghami, Z. Asgharpour, *J. Cluster Sci.* 27(2016), 1701-17018.
- [24] E. Zamanifar, F. Farzaneh, *Reaction Kinetics, Kinet. Mech. Cat.* 104 (2011) 197-209.
- [25] F. Farzaneh, Y. Sadeghi, *J. Mol. Catal. A: Chem.* 398 (2015) 275-281.
- [26] P. Van Der Voort, K. Leus, Y.-Y. Liu, M. Vandichel, V. Van Speybroeck, M. Waroquier, S. Biswas, *New J. Chem.* 38 (2014) 1853-1867.
- [27] M.J. Katz, Z.J. Brown, Y.J. Colon, P.W. Siu, K.A. Scheidt, R.Q. Snurr, J.T. Hupp, O.K. Farha, *Chem. Commun.* 49 (2013) 9449-9451.
- [28] C. Jean-Louis, *J. Quantum Chem.* 47 (1993) 101-101.
- [29] R.M. Dickson, A.D. Becke, *J. Phys. Chem.* 100 (1996) 16105-16108.
- [30] B. Vincenzo, C. Maurizio, T. Jacopo, *J. Comput. Chem.* 19 (1998) 404-417.
- [31] M.J. Frisch, G.W. Trucks, H.B. Schlegel, G.E. Scuseria, M.A. Robb, J.R. Cheeseman, V.G. Zakrzewski, J.A. Montgomery, R.E. Stratmann, J.C. Burant, S. Dapprich, J.M. Millam, A.D. Daniels, K.N. Kudin, M.C. Strain, O. Farkas, J. Tomasi, V. Barone, M. Cossi, R. Cammi, B. Mennucci, C. Pomelli, C. Adamo, S. Clifford, J. Ochterski, G.A. Petersson, P.Y. Ayala, Q. Cui, K. Morokuma, D.K. Malick, A.D. Rabuck, K. Raghavachari, J.B. Foresman, J. Cioslowski, J.V. Ortiz, B.B. Stefanov, G. Liu, A. Liashenko, P. Piskorz, I. Komaromi, R. Gomperts, R.L. Martin, D.J. Fox, T. Keith, M.A. Al-Laham, C.Y. Peng, A. Nanayakkara, C. Gonzalez, M. Challacombe, P.M.W. Gill, B.G. Johnson, W. Chen, M.W. Wong, J.L. Andres, M. Head-Gordon, E.S. Replogle, J.A. Pople, *Gaussian 98 (Revision A.1)*, Gaussian, Inc., Pittsburgh PA, 1998.
- [32] H.R. Abid, H. Tian, H.-M. Ang, M.O. Tade, C.E. Buckley, S. Wang, *Chem. Eng. J.* 187 (2012) 415-420.
- [33] X. Zhu, J. Gu, Y. Wang, B. Li, Y. Li, W. Zhao, J. Shi, *Chem. Commun.* 50 (2014) 8779-8782.

- [34] M. Lammert, C. Glißmanna, N. Stock, Dalton Trans, 2017, 46, 2425-2429.
- [35] H. Wu, Y. S. Chua, V. Krungleviciute, M. Tyagi, P. Chen, T. Yildirim, W. Zhou, J. Am. Chem. Soc. 2013, 135, 10525–10532.
- [36] G. C. Shearer, J. G. Vitillo, S. Bordiga, S. Svelle, U. Olsbye, K. P. Lillerud, Chem. Mater. 2016, 28, 7190-7193.
- [37] A. Wang, Y. Zhou, Z. Wang, M. Chen, L. Sun, X. Liu, RSC Adv. 6 (2016) 3671-3679.
- [38] Y. Luan, Y. Qi, Z. Jin, X. Peng, H. Gao, G. Wang, RSC Adv. 5 (2015) 19273-19278.
- [39] N.D. McNamara, G.T. Neumann, E.T. Masko, J.A. Urban, J.C. Hicks, J. Catal. 305 (2013) 217-226.
- [40] M. Pourkhosravani, S. Dehghanpour, F. Farzaneh, Catal Lett, 2016, 146, 499–508.
- [41]. P. Yang, Q. Liu, J. Liu, H. Zhang, Z. Li, R. Li, L. Liu , J. Wang, J. Mater. Chem. A, 2017, 5, 17933–17942.
- [42] R. G.S. Millan, E. L. Maya, M. Hall, N. M. Padial, G. W. Peterson, J.B. D. Coste, L. M. R. Albelo, J. E. Oltra, E. Barea, J. A. R. Navarro, ACS Appl. Mater. Interfaces 2017, 9, 23967–23973.
- [43] Y. Cao, H. Zhang , F. Song , T. Huang , J. Ji , Q. Zhong , W. Chu, Q. Xu, Materials, 2018, 11, 589.
- [44] J. Ding, Z. Yang, C. He, X. Tong, Y. Li, X. Niu, H. Zhang, J. Colloid Interface Sci. 497 (2017) 126-133.
- [45] J. Navarrete, M. A. Ramírez, P. Schacht, L. Schacht, J. Mex. Chem. Soc. 54 (2010), 69.
- [46] V. Mazzieri, F. Coloma-Pascual, M. González, P. L'argentičre, N. Fígoli, React. Kinet. Catal. Lett. 76 (2002) 53-59.
- [47] S. Bordiga, C. Lamberti, G. Ricchiardi, L. Regli, F. Bonino, A. Damin, K.P. Lillerud, M. Bjorgen, A. Zecchina, Chem. Commun. (2004) 2300-2301.
- [48] W. Lin, H. Frei, J. Am. Chem. Soc. 127 (2005) 1610-1611.
- [49] Alamgir, W. Khan, S. Ahmad, M. Mehedi Hassan, A.H. Naqvi, Opt. Mater, 38 (2014) 278-285.
- [50] J. Tauc, R. Grigorovici, A. Vancu, Phys. Status Solidi B, 15 (1966) 627-637.
- [51] S. Øien, D. Wragg, H. Reinsch, S. Svelle, S. Bordiga, C. Lamberti, K.P. Lillerud, Cryst.

- Growth Des. 14 (2014) 5370-5372.
- [52] J. Liu, F. Wang, S. Qi, Z. Gu, G. Wu, New J. Chem. 37 (2013) 769-774.
- [53] L.M. Slaughter, J.P. Collman, T.A. Eberspacher, J.I. Brauman, Inorg. Chem. 43 (2004) 5198-5204.
- [54] A. Rezaeifard, I. Sheikhshoae, N. Monadi, M. Alipour, Polyhedron, 29 (2010) 2703-2709.
- [55] Z. Azarkamanzad, F. Farzaneh, M. Maghami, J. Simpson, M. Azarkish, Appl. Organomet. Chem. 2018, 32, e4168, <https://doi.org/10.1002/aoc.4168>.
- [56] C. Reichardt, Solvents and Solvent Effects in Organic Chemistry third ed., 2003  
WILEY-VCH Verlag GmbH & Co. KGaA, Weinheim

### Figure Captions:

**Fig. 1.** The XRD spectra of (a) UiO-66(Zr) and (b) UiO-66(Zr)-V c) UiO-66(Zr)-V after reaction.

**Fig. 2.** EDS image of a) UiO-66(Zr) b) UiO-66(Zr)-V.

**Fig. 3.** The FTIR spectra of a) UiO-66(Zr) and b) UiO-66(Zr)-V.

**Fig. 4.** TGA curves of the a) UiO-66(Zr) and b) UiO-66(Zr)-V.

**Fig. 5.** The Raman spectra of a) UiO-66(Zr) and b) UiO-66(Zr)-V.

**Fig. 6.** Nitrogen adsorption–desorption isotherms at 77 K for a) UiO-66(Zr) and b) UiO-66(Zr)-V.

**Fig. 7.** The XPS spectra of UiO-66(Zr)-V sample: (a) survey scan, (b) Zr 3d, (c) V 2p, (d) O 1s and (e) Cl 2p.

**Fig. 8.** Comparison between X-ray and optimized structure (a) six-center octahedral zirconium oxide cluster, b) optimized  $[\text{Zr}_6\text{O}_4(\text{OH})_4]$  cluster at B3LYP/6-31G\*\* level.

**Fig. 9.** Proposed reaction path between of vanadium (V) and  $[\text{Zr}_6\text{O}_4(\text{OH})_4]$  cluster (A, B, C) to form different complexes including (I) to (V).

**Fig. 10.** The relative energy diagram of different proposed compounds (I, II, III, IV and V).

**Fig. 11.** The solvent effect on the conversion and selectivity of trans-2-hexen-1-ol using UiO-66(Zr)-V as catalyst.

**Fig. 12.** Conversion and selectivity of of trans-2-hexen-1-ol with different amounts of the UiO-66(Zr)-V as catalyst in different times of reaction.

**Fig. 13.** The effect of recycling of UiO-66(Zr)-V catalyst on epoxidation of trans-2-hexen-1-ol, under optimum condition.

Table 2: Comparison between some selected experimental (Exp.) and calculated (The.) geometrical parameters of  $[\text{Zr}_6\text{O}_4(\text{OH})_4]$  cluster.

Connected atom	Exp.	The.
Bond distance (Å)		
Zr4-O5	2.261	2.267
Zr4-O2	2.261	2.340
Zr6-O7	2.261	2.268
Zr6-O11	2.261	2.300
Zr6-O13	2.261	2.310
Zr8-O7	2.261	2.307
Zr9-O11	2.261	2.303
Zr9-O2	2.261	2.268
Zr9-O13	2.261	2.286
Zr10-O7	2.261	2.217
Zr10-O12	2.261	2.252
Standard deviation		0.13
Bond angle (°)		
O2-Zr1-O14	76.60	72
O14-Zr4-O5	76.60	72
O5-Zr4-O14	76.60	71.98
Zr1-O14 –Zr9	102.27	99.38
Zr10-O11 –Zr6	102.28	108.16
Standard deviation		10.32

**Table1.** Textural properties and ICP of UiO-66(Zr) and UiO-66(Zr)-V materials.

Material	$S_{\text{BET}}(\text{m}^2\text{g}^{-1})$	Mean pore diameter (nm)	Total pore volume ( $\text{cm}^3\text{g}^{-1}$ )	ICP (Zr) (wt%)	ICP (V) (wt%)
UiO-66(Zr)	1068.3	2.2346	0.5968	28.45	-----
UiO-66(Zr)-V	1019.5	2.3388	0.5961	27.94	5.76

**Table 3.** Thermodynamic data for the different complexes, including enthalpies ( $\Delta H_{\text{com}}$ ), Gibbs free energies ( $\Delta G_{\text{com}}$ ) and entropies ( $\Delta S_{\text{com}}$ ).

	<sup>a</sup> $\Delta E_{\text{Com}}^{\text{Sin}}$	<sup>b</sup> $\Delta E_{\text{Com}}$	<sup>c</sup> $\Delta H_{\text{Com}}$	<sup>d</sup> $\Delta G_{\text{Com}}$	$\Delta S_{\text{Com}}$
Complex I	-109.23	-94.901	-95.491	-88.5354	-0.024
Complex II	-102.71	-93.017	-93.607	-88.39585	-0.021
Complex III	-63.12	-46.777	-47.367	-43.14845	-0.017
Complex IV	-60.0	-45.070	-45.660	-41.6896	-0.016
Complex V	-12.24	5.758	5.168	10.87545	-0.023

<sup>a</sup> $\Delta E_{\text{com}}^{\text{Sin}}$  at B3LYP/6-311++G\*\* level,

<sup>b</sup> $\Delta E_{\text{com}} = E_{\text{opt}} [\text{Zr}_6\text{O}_4(\text{OH})_4]\text{-V} - (E_{\text{opt}} [\text{Zr}_6\text{O}_4(\text{OH})_4] + E_{\text{opt}} \text{v})$  at hf/3-21g level

<sup>c</sup> $\Delta H_{\text{com}} = \Delta E + \Delta nRT$ , <sup>d</sup>  $\Delta G_{\text{com}} = \Delta H - T\Delta S$

**Table 4.** Selected some bond lengths (Å) and bond angles (°) of  $[\text{Zr}_6\text{O}_4(\text{OH})_4]\text{-V}$  complex.

<b>Bond distance (Å)</b>	
<b>Zr1- O14</b>	2.350
<b>Zr8- O14</b>	2.141
<b>Zr8-O15</b>	1.793
<b>Zr1-O16</b>	1.789
<b>V22-O15</b>	2.140
<b>V22-O16</b>	2.133
<b>Bond angle (°)</b>	
<b>O3-Zr1-O16</b>	61.71
<b>O14-Zr8-O15</b>	89.19
<b>Zr1- O3-Zr8</b>	86.65
<b>Zr1- O16-V22</b>	124.47
<b>Zr8- O15- V22</b>	104.49
<b>O16- V22-O16</b>	113.52

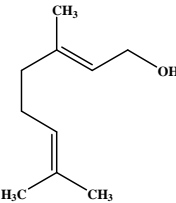
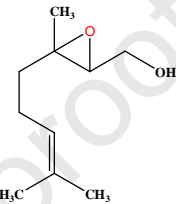
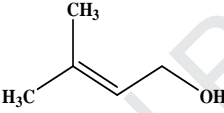
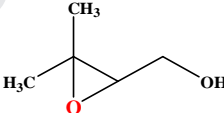
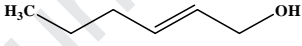
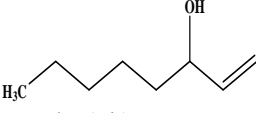
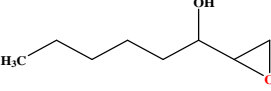
**Table 5.** Conversion and selectivity of of trans-2-hexen-1-ol with different amounts of the UiO-66-V as catalyst in different times of reaction <sup>a</sup>.

Reaction time	1 h	3 h	5 h	7 h	9h	11h
Amounts of catalyst (mg)	Conv. (%) (Sel. (%)) <sup>b</sup>					
<b>10</b>	12 (100)	21 (100)	26 (100)	32(100)	44(100)	52(100)
<b>30</b>	18 (100)	39 (100)	56 (100)	68 (100)	88 (100)	91(100)
<b>50</b>	15 (100)	27 (100)	29 (100)	58 (100)	58 (100)	56(100)

<sup>a</sup> Reaction conditions: 10,30 and 50 mg cat, 10 mmol trans-2-Hexen-1-ol, 12 mmol 70 wt% TBHP, 5 mL CH<sub>3</sub>CN.

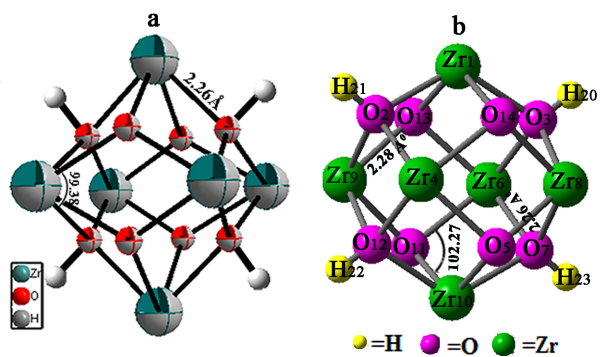
<sup>b</sup> Conversion (%) and selectivity (%) were determined by GC and GC-Mass with an internal standard method.

**Table 6.** Results obtained for epoxidation of different allyl alcohols in the Presence of UiO-66(Zr)-V as catalyst.

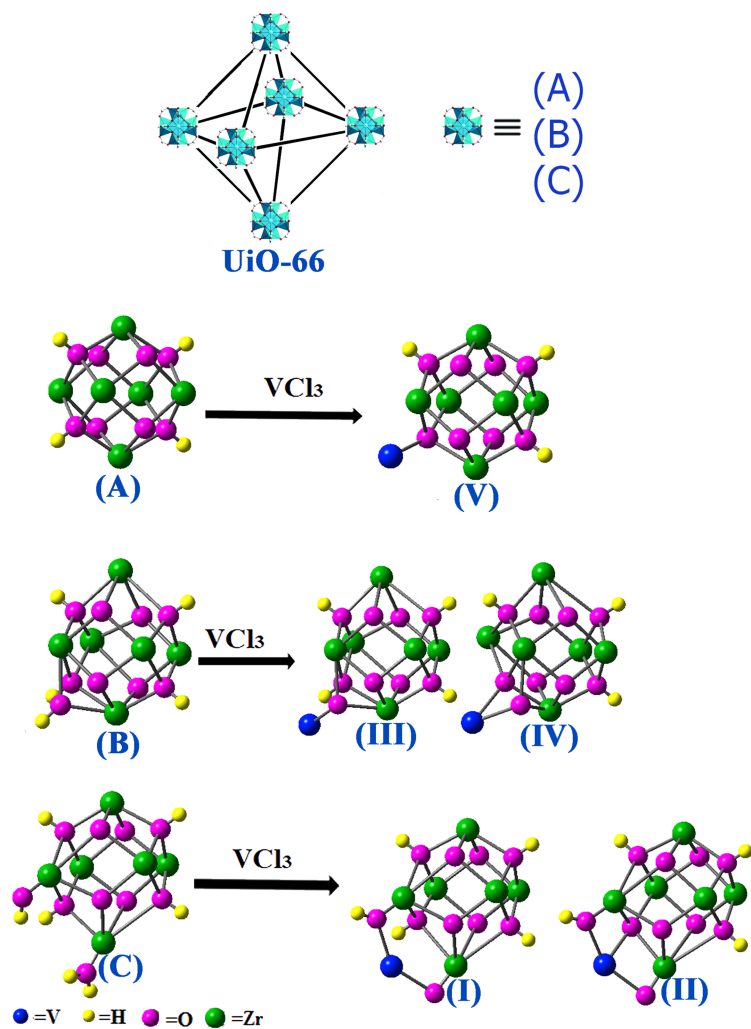
Entry	Substrate conversion(%) (Time)	Epoxide selectivity (%) (TON) <sup>b</sup>
1	 87 (7h)	 100 (256)
2	 97 (11h)	 100 (286)
3	 88 (9h)	 100 (259)
4	 46 (7h)	 100 (135)

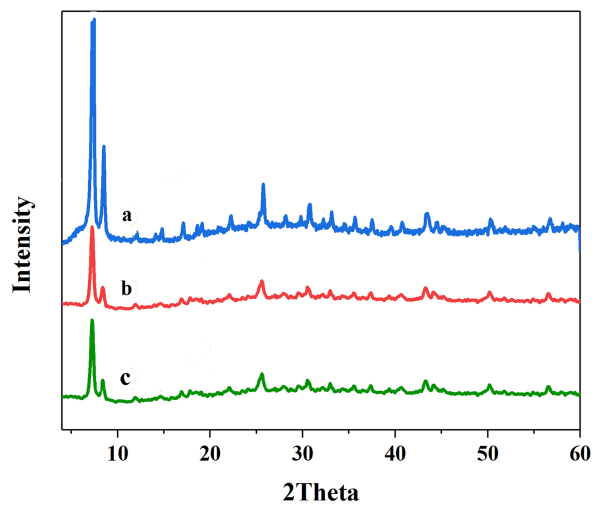
<sup>a</sup> Reaction conditions: 30 mg, catalyst, substrate (allyl alcohols, 10 mmol), TBHP (12 mmol), solvent (acetonitril, 5 ml, reflux at 80 °C).

<sup>b</sup>TON is the mmol of product to mmol of vanadium present in catalyst.

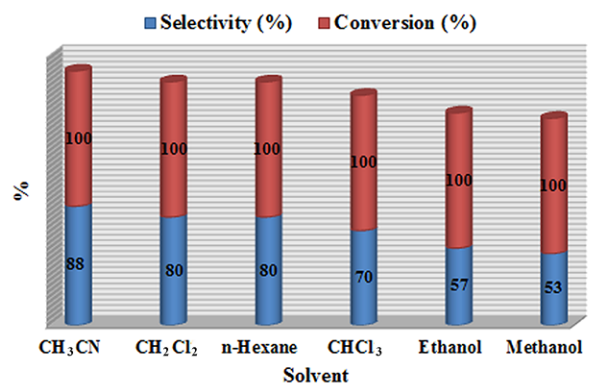


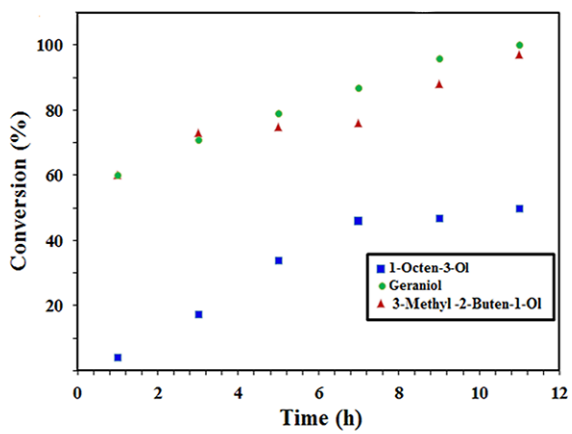
Journal Pre-proof



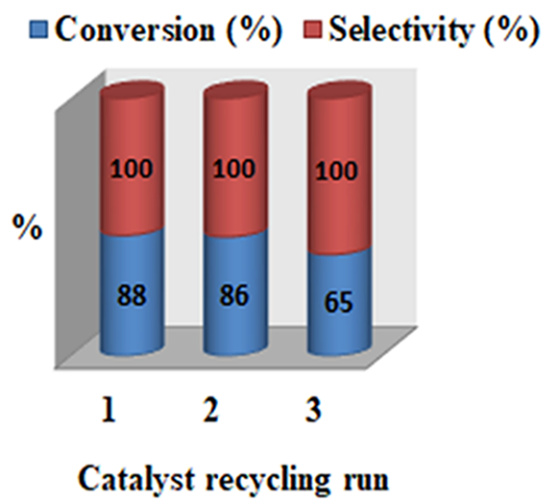


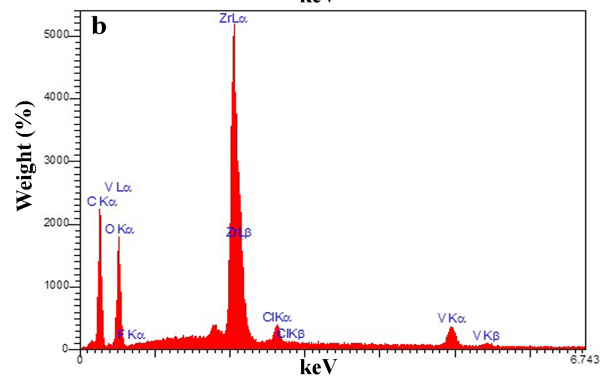
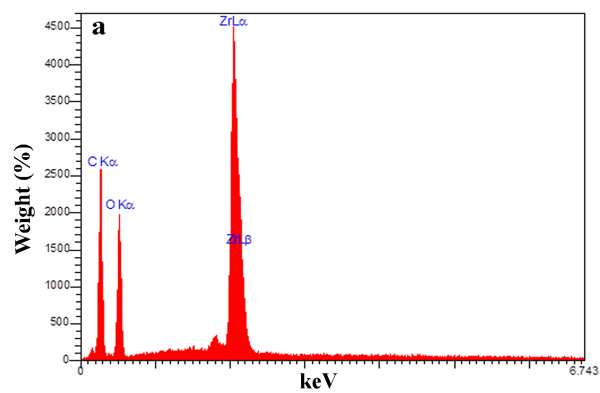
Journal Pre-proof

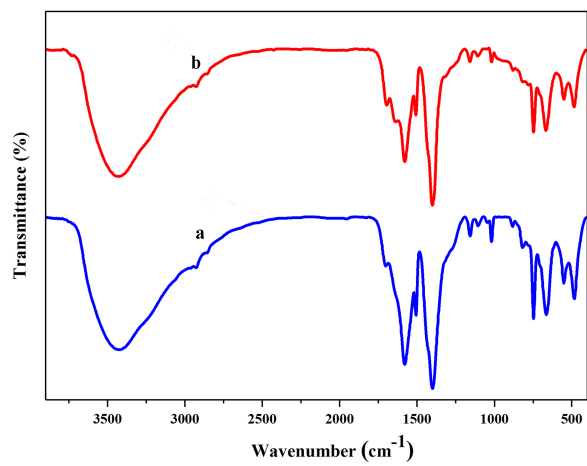




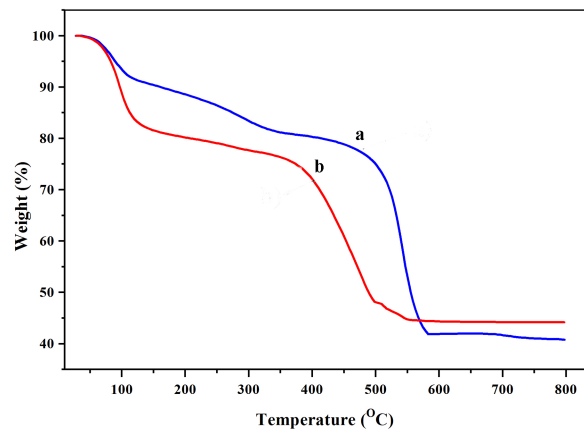
Journal Pre-proof

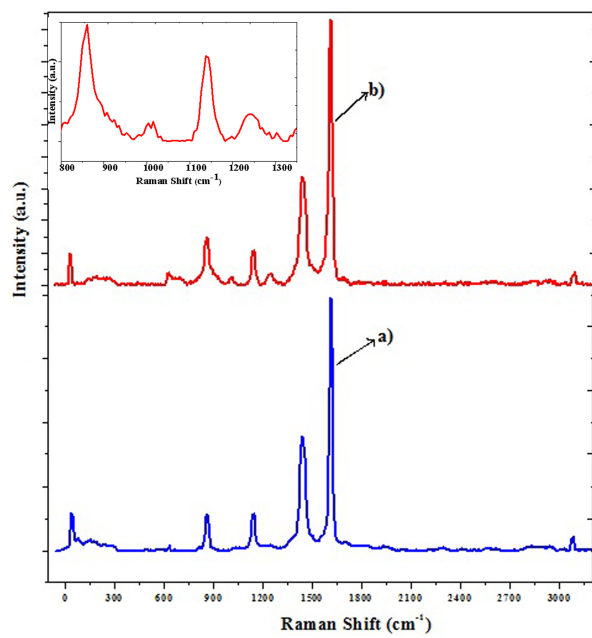


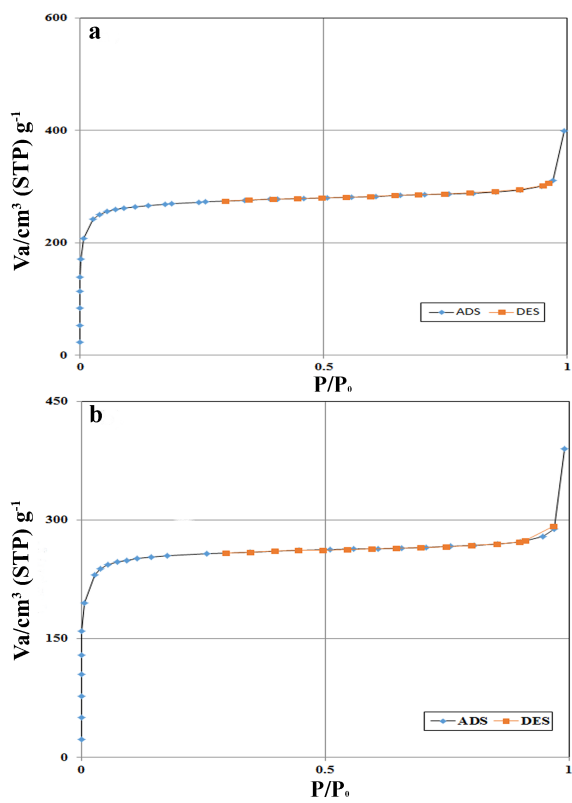


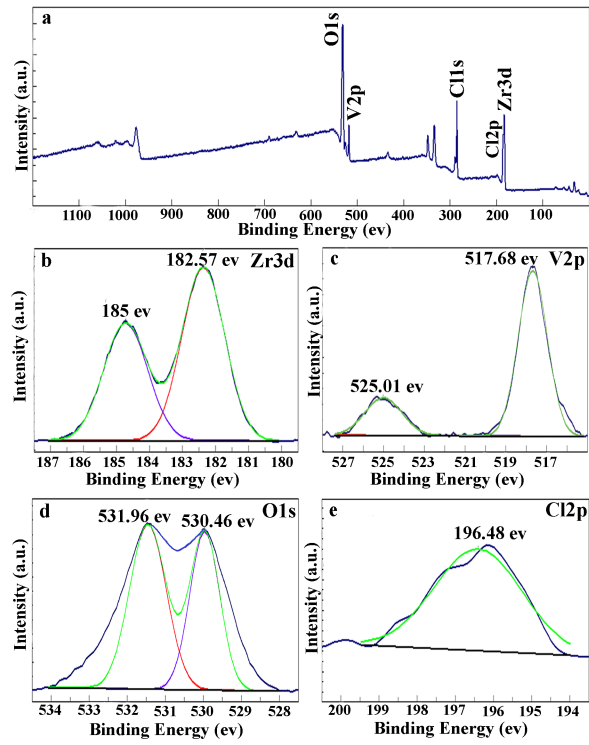


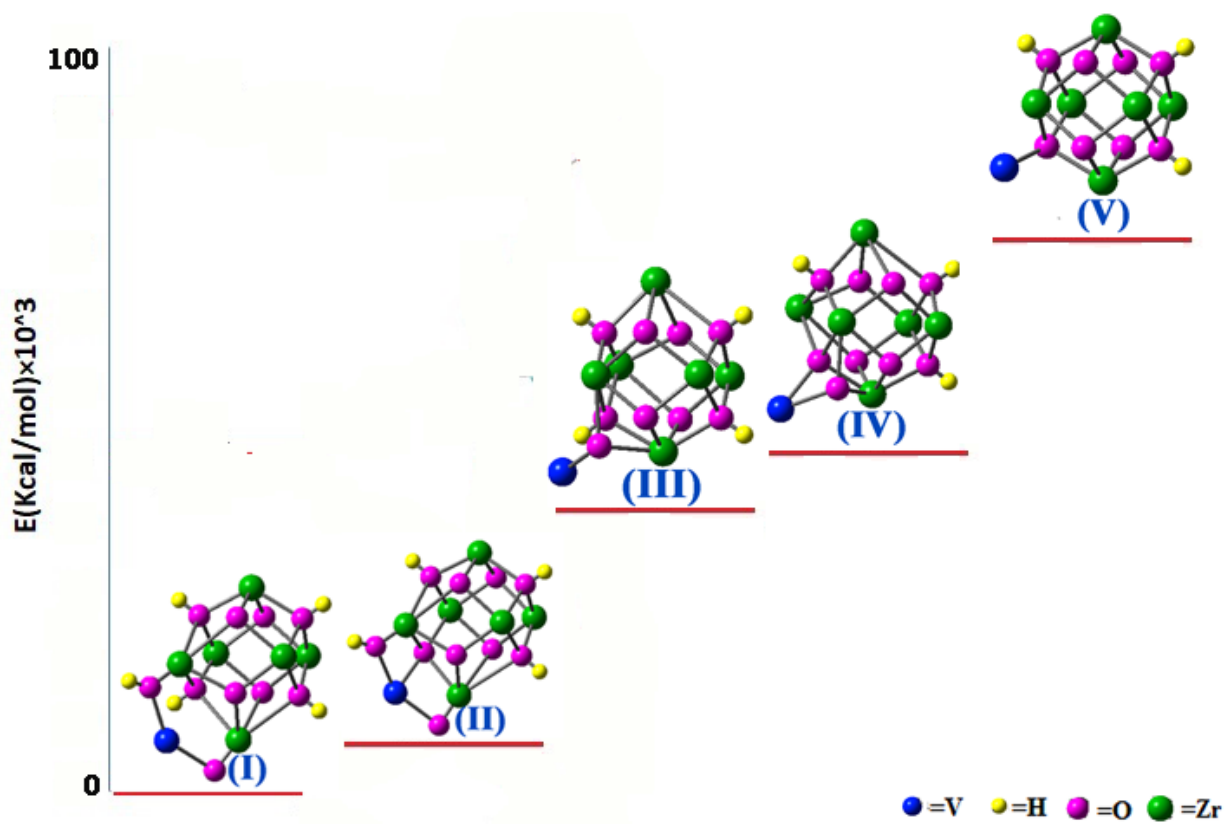
Journal Pre-proof











**Highlights:**

- ◆ The metal organic framework UiO-66(Zr)-V was prepared by metalation of the UiO-66(Zr) nodes with  $VCl_3$ .
- ◆ Utilization the density functional theory (DFT) was used in order to find the most stable position of the vanadium of metallated UiO-66(Zr).
- ◆ The catalytic activity of UiO-66(Zr)-V on the epoxidation of allyl alcohols is considerable.